PERGAMON

International Journal of Heat and Mass Transfer 45 (2002) 4033–4043

International Journal of HEAT and MASS TRANSFER

www.elsevier.com/locate/ijhmt

Effects of spray characteristics on critical heat flux in subcooled water spray cooling

Ruey-Hung Chen *, Louis C. Chow, Jose E. Navedo

Department of Mechanical, Materials and Aerospace Engineering, University of Central Florida, 4000 Central Florida Boulevard, Orlando, FL 32816-2450, USA

Received 25 April 2001; received in revised form 15 November 2001

Abstract

Effects of spray parameters (mean droplet size, droplet flux, and droplet velocity) on critical heat flux (CHF) were studied while these parameters were systematically varied. The effect of each parameter was studied while keeping the other two nearly constant. The mean droplet velocity (V) had the most dominant effect on CHF and the heat transfer coefficient at CHF (h_c), followed by the mean droplet flux (N). The Sauter mean diameter (d_{32}) did not appear to have an effect on CHF. By increasing V, CHF and h_c were increased. This trend was observed when all other spray parameters were kept within narrow ranges and even when relaxed to wider ranges, indicating the dominant effect of V. The effect of N, although not so much as V, was also found to be significant. Increasing N resulted in an increase in CHF and h_c when other parameters are kept in narrow ranges. A dilute spray with large droplet velocities appears to be more effective in increasing CHF than a denser spray with lower velocities for a given N. The mass flow rate was not a controlling parameter of CHF.

Keywords: Spray cooling; Nucleate heat transfer; Boiling

1. Introduction

The success of many industrial applications requires the ability to remove high heat fluxes. These applications are in the cooling of increasingly high-speed electronic components [1] and high-power lasers [2]. Such needs will not be met by the limited capability of conventional cooling techniques such as forced convection. Heat transfer techniques involving phase change processes are likely to play an important role, as they take advantage of relatively large values of latent heat. With phase change, heat removal can be achieved with only a small surface superheat, which is desirable for stabilizing the performance of microelectronic devices. The heat flux by pool boiling of water can reach approximately 120 W/cm^2. Spray cooling holds even greater promise because it offers high heat transfer coefficients and critical heat flux (CHF) typically an order of magnitude higher than pool boiling for liquids including water, FC-72 and liquid nitrogen (LN_2) [3–12]. It is known that in spray cooling the value of CHF varies over a wider range for a given heater, depending on the spray characteristics such as N, V and d_{32} [6,11].

A spray consists of liquid droplets generated by a pressure- or air-assisted atomizer that impinge on a heated surface [13]. Spray has been used to cool highly heated surfaces, such as those in steel mills, where film cooling rather than nucleate boiling dominates. Recent research of spray cooling involves a significant portion of heat transfer that is due to nucleate boiling heat transfer. Several events occur in nucleate boiling in such a spray cooling technique. The impacting droplets puncture and remove the vapor bubble (or the nucleus), while forming a thin liquid layer on the heated surface. The bubble size at puncture is usually smaller than the departure under pool boiling conditions. Some of these bubbles are the surface nuclei, while the others are the so-called secondary nuclei. Secondary nuclei are generated when air or vapor is entrained by the droplets into

* Corresponding author. Tel.: +1-407-823-3402; fax: +1-407-823-0208.

E-mail address: chenrh@pegasus.cc.ucf.edu (R.-H. Chen).

0017-9310/02/$ - see front matter
PII: S0017-9310(02)00113-8

Nomenclature

CHF (or q''_c)	critical heat flux
d	mean droplet diameter
d_{32}	Sauter mean diameter
G	liquid flow rate on heater surface
h	convection heat transfer coefficient, $q''/(T_w - T_\infty)$
h_c	convection heat transfer coefficient at CHF, $q''_c/(T_{w,CHF} - T_\infty)$
h_{fg}	latent heat of evaporation
N	mean droplet flux ($= nV$)
n	mean droplet number density
P	gage pressure at nozzle
q''	heat flux
r	radial coordinate
$T_{w,CHF}$	surface temperature at CHF
T_{sat}	saturation temperature of liquid
T_w	surface temperature
T_∞	liquid temperature at nozzle exit
V	mean droplet speed
ΔT	surface superheat ($= T_w - T_{sat}$)
x	streamwise coordinate

the thin liquid film [10,13]. The heat transfer mechanism is believed to consist of three key mechanisms: (1) nucleate boiling due to both surface and secondary nuclei [11], (2) convective heat transfer, and (3) direct evaporation from the surface of the liquid film [14–17]. A recent investigation of the heat transfer mechanism in spray cooling can be found in Rini et al. [10]. The heat transfer enhancement can be attributed to the abovementioned three mechanisms.

In the study of Rini et al. [10], the controlled spray characteristic was the droplet flux (N). It was pointed out [6] that other spray characteristics might directly affect the relative importance of the three heat transfer mechanisms. However, no systematic investigation has been carried out by independently varying each of the spray parameters. The spray parameters include mass flux (G), mean droplet velocity (V), droplet number flux (N), droplet number density (n), and the Sauter mean diameter of droplets (d_{32}). Nonetheless, only three of these five parameters are independent variables, as $N = nV$ and $G \approx \rho\pi d_{32}^3 N/6$. This study focuses on the effects of spray characteristics on the heat transfer coefficient and critical heat flux (CHF). The effect of surface conditions on CHF were eliminated or significantly reduced by using the same surface preparation procedure. A literature review is outlined below, which helps to further clarify the motivation of this study.

Toda and Uchida [15–17] experimented with water sprays at low flow rates and showed that values of CHF of 250 W/cm^2 were consistently obtained at ΔT ranging from 30 to 60 K. The spray parameters (i.e., N, d_{32}, V) were not measured in that study. However, Toda estimated that the water droplet velocity ranged from 50 to 100 m/s, and that the mean droplet diameter ranged from 200 to 700 μm. It was shown that q'' was not sensitive to V over the velocity range of approximately 2.0–7.0 m/s [17]. This finding contradicts that by Monde [18], that CHF increased with increasing V. It is noted that Toda, Uchida and Monde investigated sprays of low flow rates, for which nucleate heat transfer might not exist.

Tilton [19], using pressure-atomized water sprays, obtained heat fluxes up to 1000 W/cm^2 at surface superheat of < 40 K. The average droplet diameter and the mean velocities in that study were approximately 80 μm and 10 m/s, respectively. Tilton concluded that while decreasing d_{32} increases h (the heat transfer coefficient), the mass flow rate (G) may not be a factor in controlling CHF. In another study using water by Toda [15], CHF was found to increase by approximately 50% as the droplet diameter was increased from 88 to 120 μm. Halvorson et al. [20] pointed out that using water droplet of sizes from 2300 to 3800 μm, without detailed knowledge of N, V, or G, would only produce a CHF around 120 W/cm^2, similar to the CHF of pool boiling. Both Pais et al. [5] and Estes and Mudawar [9] suggested that CHF could be increased by decreasing the droplet diameter. Sehmbey et al. [8] showed that smaller droplets can produce same values of CHF at smaller flow rates as larger droplets at larger flow rates. These results of the dependence of CHF on droplet size are conflicting, as the spray parameters were not isolated for a systematic investigation.

There exists evidence that CHF increases with increasing spray mass flux [5,9,18]. Based on a limited set of experiments, where spray parameters were not independently varied, it was concluded that CHF is largely dependent on the spray mass flux impacting the heater surface. As reviewed in a recent article by Chow et al. [13], the value of CHF can be relatively independent of the mass flow rate that was varied by a factor of three. Such a result can be seen in Fig. 1 [8], where data along each straight line were obtained for a given nozzle. Along each straight line, the droplet diameter was maintained constant while it increased from left to right in Fig. 1. However, spray parameters were not independently isolated along each line. While it is clear from Fig. 1 that for a given nozzle CHF increases with increasing

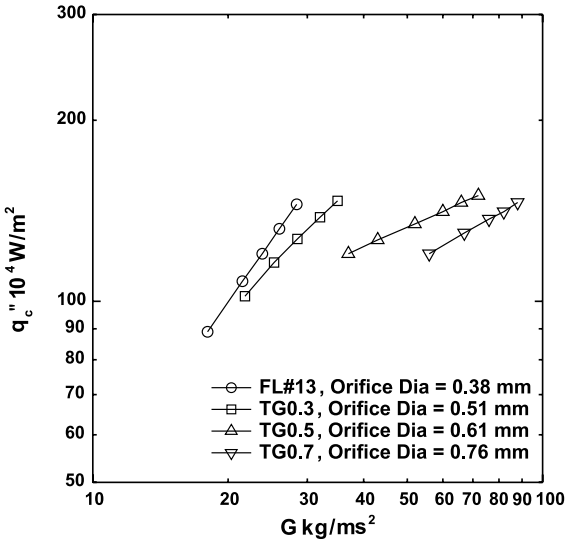

Fig. 1. Effects of spray characteristics on critical heat flux in subcooled water spray cooling.

G, same values of CHF can be obtained by using different nozzles that produce different values of G. This indicates a strong dependence of the CHF on parameters other than simply the mass flow rate.

To the authors' knowledge, the study performed herein is the first that independently varies each of V, N, and d_{32} and assesses their contribution to spray cooling heat transfer. It is noted that in this study all of these spray parameters are ensemble averages. While this report is concentrated on spray cooling in the nucleate heat transfer regime, spray cooling also find applications in cooling surfaces at temperatures above the Leidenfrost point. A recent review on the progress in this area can be found in Ref. [21]. Studies using mono-dispersed droplets were previously conducted to investigate effects of spray parameters on heat transfer, but were mostly concerned with film boiling [22–24].

2. Experiment

The heater was made of a pure copper block. It was heated by four 500-W cartridge heaters positioned as shown in Fig. 2. The copper block was a solid cylinder 12-cm in diameter and 30.5 cm in height that tapered off near the top to a 1×1 cm^2 crown at the top. It was supported by an aluminum enclosure and was surrounded by Durablanket© insulation (thermal conductivity, $k = 0.013$ W/m K) placed between the copper and the aluminum enclosure. Thus, the entire copper block was insulated except the crown (i.e., the heater surface). This apparatus was capable of supplying more than 1500 W to the 1 cm^2 crown surface. The space between the crown/heater surface and the aluminum enclosure was sealed using a high-temperature silicon rubber sealant so that the water could not reach the copper block.

Three K-type thermocouples (TC1, TC2 and TC3 in Fig. 2, each having a 0.003 in. bead diameter) were imbedded below the heater surface (in the neck region) to provide the temperature gradient and temperature profile within the neck region. Knowing the temperature difference between these thermocouples and the distance between them (0.37 cm), it was possible to predict the heat flux using the one-dimensional Fourier's law of

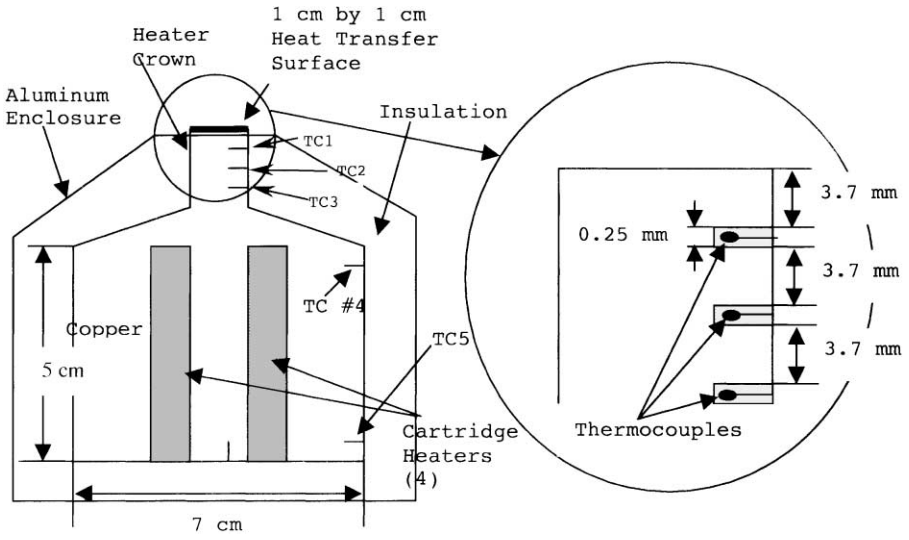

Fig. 2. Sketch of heater.

heat conduction. The distance between the heater surface and TC1 is also 0.37 cm. The surface temperature was determined by extrapolation using the measured temperature gradient in the neck region specified by the three thermocouples. Although the temperature of the heater block changed as the heat input was increased during the experiment, the temperature at the crown reached a quasi-steady-state due to the fact that the amount of heat stored in the crown region was very small. This was verified by the fact that the heat flux calculated from TC1 and TC2 readings was equal to that calculated from TC2 and TC3 readings. Two thermocouples (TC4 and TC5 in Fig. 2) were placed on the large part of the copper block to monitor the temperatures so that an automatic shut-off of power could be accomplished when the temperatures approached near the operational limit (i.e., the softening point) of the heater system. The softening points were 800 and 1000 °C for the cartridge heaters and copper, respectively. A computer recorded the temperature measurements and calculated the heat flux and the surface temperature.

Before fabricating the heater, a finite element analysis of the steady-state heat conduction in the heater block was performed, using a software package ANSYS, to ensure (1) the softening points of the materials used were not exceeded and (2) that the isotherms in the neck region were one-dimensional, allowing easy determination of q'' and T_w.

For heat transfer experiments, the spray nozzle was positioned directly above and perpendicular to the horizontally placed heater surface. Water at room temperature ($T_\infty = 25$ °C) was pumped from a reservoir to the spray nozzle. The nozzle pressure (P, in psig) produced by a gear pump was read by a pressure gauge. Each experiment (i.e., for one q'' vs. ΔT curve) was run with a nozzle at a specific pressure and distance from the heated surface. The experiment was conducted in the open laboratory environment.

For this study, it is essential to satisfy the following criteria. First, there needed to be large variations in N, d_{32}, and V so that a database could be constructed that would contain nearly independent variation in each of the spray parameters while keeping the other two in narrow (i.e., nearly fixed) ranges. Secondly, it was necessary that these parameters of interest were radially uniform (i.e., one-dimensional) at known distances from the nozzle exit. The values of N, d_{32}, and V were measured using a Dantec PDPA system without the presence of the heater. Effects of the presence of the heater were discussed by Tilton [19], including complicated patterns of liquid droplets rebounding from the surface. It is noted that results of these cold spray measurements will be different than those measured right above the heated surface. However, these values are more practical to use because one can design atomizers with spray parameters that will optimize the spray cooling heat transfer. These three spray parameters were determined for each combination of the nozzle type, the nozzle pressure (P), and the distance from the nozzle (x). It is noted that with the same nozzle, the measured values of N and V were different at different distances. Droplet might also coalesce in the flow direction, causing d_{32} to vary with x. However, relationships between d_{32} and x were outside of the scope of this study. More than 3000 combinations of the three spray parameters were obtained. However, only subsets satisfying the above criteria were adopted for the heat transfer experiment. The details for obtaining such subsets are tedious and the reader is referred to Ref. [25]. Typical radial profiles for N, d_{32}, and V are shown in Fig. 3, respectively, while those for other subsets are similarly. The radial profiles illustrate the radial uniformity (within about 5% over the area corresponding to the heater surface, $r = 0.5$ cm), satisfying the one-dimensional requirement mentioned above. It is further noted that more than 20 full-cone nozzles were used. These nozzles were commercially available from three industrial suppliers: Hago (B-series nozzles, described below), Bete and Delavan.

The characteristics of the heater surface are known to affect results of boiling heat transfer [7,13]. The following procedure was followed, at the commencement of each day's experiments, to ensure consistency in the surface properties of the heater. First, the surface was cleaned with acetone to remove oxides and residues from water. It was then polished with 600-grit, followed by 1000-grit, sandpapers. The RMS surface roughness was measured by a profilometer to be consistently about 4 μm.

For each experiment, the power to the heater block was gradually increased at a slow rate. CHF was determined to be the heat flux above which excursion in T_w

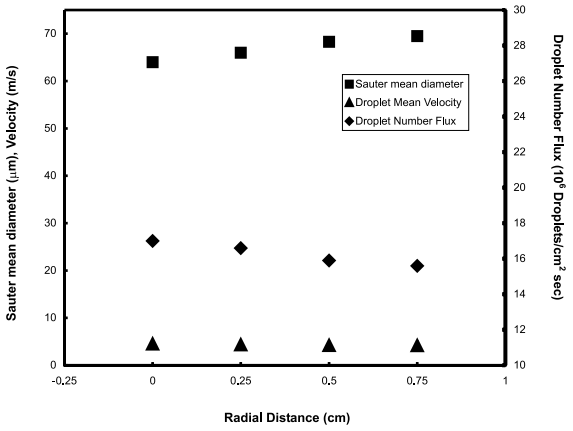

Fig. 3. Typical radial profiles of spray parameter over the extent of the heater surface, whose edge is at $r = 0.5$ cm. It is noted that the spray parameters of interest fall within narrow ranges, giving a nearly one-dimensional spray.

occurred. When CHF was reached, the power to the heater was turned off and the spray was continuously supplied until the heater block cooled down to room temperature. Then, a new combination of the nozzle, P, and x was implemented and the above steps were repeated. Results of q'' vs. ΔT were repeatable after two initial runs (see Fig. 4). It was after the initial three runs that the reported experimental results were obtained. Therefore, the reported variation in the heat transfer and CHF results were caused by variations in the spray characteristics rather than by changes in the surface conditions.

The uncertainty in q'' is a function of x, T, and k, because $q'' = -k\Delta T/\Delta x$ (Fourier's law). It is given by the equation

$$\omega q'' = [(\partial q''/\partial x)\omega_x]^2 + [(\partial q''/\partial T)\omega_T]^2 + \{[(\partial q''/\partial k)\omega_k]^2\}^{1/2},$$

where ω denote the uncertainty in the parameter that appears as the subscript and q'', x, T, and k denote the heat flux, position of TCs, temperature and thermal conductivity, respectively. The uncertainty in x is assumed to be half of the bead diameter of the thermocouple (i.e., 0.125 mm). ω_T is 2.0 °C, as given by the manufacturer. ω_k was determined from thermophysical tables from several sources and was determined to be 0.05 W/m K. $\omega_{q''}$ thus determined is about 5.5 percent at 1000 W/cm^2. The surface temperature T_w was determined by again using $q'' = -k\Delta T/\Delta x$ extrapolating from temperature measured at TC1. The uncertainty of T_w was then calculated to be about 3.0 °C.

The Dantec PDPA Manual [26] gives the uncertainty in the PDPA measurements. The uncertainty in the droplet velocity is less than 5 percent for droplet velocities > 4.0 m/s, which was of interest in this study. The uncertainty in the diameter measurement is also less than 5 percent. The measured number density (n) is estimated to be accurate to within 30 percent. The PDPA measurements yield the mass flow rate according to $G \sim \rho\pi d_{32}^3 nV/6$. The comparison with the measured flow rate indicated excellent agreement, to within 10%. The direct measurement of mass flow rates was performed using a graduated cylinder and a stopwatch.

3. Results and discussion

Results shown in Fig. 4 also demonstrate typical heat transfer curves (q'' vs. ΔT). The amount of heat transfer for $\Delta T = 0$ could be attributed to the single-phase convection because the liquid exiting the nozzle was at room temperature (i.e., $T_\infty = 25$ °C). Similar results under different spray conditions were observed, with the single-phase convection heat transfer contributing approximately 200 ± 50 W/cm^2, which is less than or about 1/3 of CHF values reported in this study. For simplicity, only values of CHF, instead of the heat transfer curves, will be reported. Visual inspection of the heater surface near CHF would suggest that partial dryout occurred.

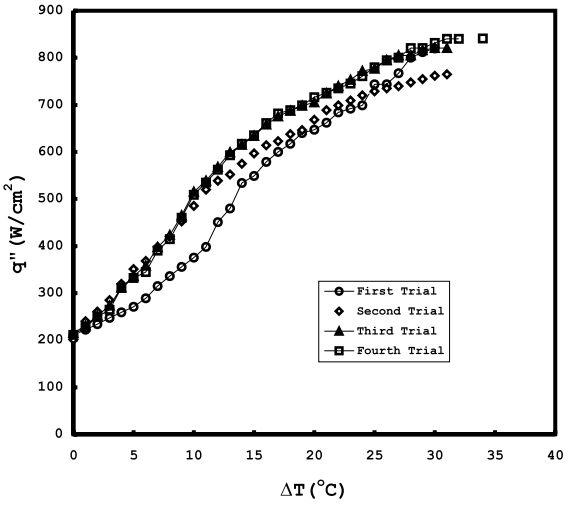

Fig. 4. Typical heat transfer curves demonstrating the repeatability after the third run. All reported CHF values in this paper were taken at end of the third run.

It is noted that the effect of G, although not an independent parameter, is also discussed. The discussion is aim to clarify the effect of G discussed in the Section 1, in addition to those of N, d_{32}, and V, which are the goal of this study.

3.1. Effects of the droplet number flux (N)

Two sets of data illustrating effects of the droplet flux (N) on CHF can be seen in Tables 1 and 2. To obtain the first set of data (Table 1), N was varied from 7.30 ×

Table 1
Experimental conditions and results of varying N while keeping d_{32} within 56 μm ± 3% and V within 7.5 m/s ± 10%

Nozzle type	B37	B50	Bete#2
Location, x (cm)	2.5	3.0	6.0
Pressure, P (psi)	50.0	100.0	60.0
N (1/cm^2 s)	7.30×10^6	15.25×10^6	29.00×10^6
G (kg/cm^2 s)	0.00072	0.00224	0.00248
d_{32} (μm)	57.3	55.4	54.7
V (m/s)	6.9	7.3	8.0
CHF (W/cm^2)	610.7	761.9	780.2
$T_{w,CHF} - T_\infty$ (K)	102.8	108.7	109.1
h_c (W/cm^2 K)	5.94	7.01	7.15

Table 2
Experimental conditions and results of varying N while keeping d_{32} within 76 μm ± 5% and V within 10.5 m/s ± 5%

Nozzle type	B37	B150	B50
Location, x (cm)	6.5	6.0	8.5
Pressure, P (psi)	90.0	60.0	160.0
N (1/cm^2 s)	5.52×10^6	17.40×10^6	18.83×10^6
G (kg/cm^2 s)	0.00146	0.00348	0.00376
d_{32} (μm)	79.7	72.6	72.6
V (m/s)	10.8	11.1	10.1
CHF (W/cm^2)	591.2	694.6	673.2
$T_{w,CHF}-T_\infty$ (K)	100.9	104.2	103.9
h_c (W/cm^2 K)	5.86	6.67	6.48

10^6/cm^2 s to 29.00×10^6/cm^2 s (by a factor of 4.2), while d_{32} and V were kept in narrow ranges 56 μm ± 2% and 7.5 m/s ± 7%, respectively. It is seen that CHF increased from 610.7 to 780.2 W/cm^2, about 30%, over the increase in N (see Table 1). The heat transfer coefficient at CHF ($h_c = q''_{CHF}/(T_{w,CHF} - T_\infty)$), increased correspondingly from 5.94 to 7.15 W/cm K, approximately 20%.

The second set of data is shown in Table 2, where N was increased from 5.52×10^6/cm^2 s to 17.40×10^6/cm^2 s and then to 18.83×10^6/cm^2 s (by a factor of about 3), while d_{32} and V were kept in narrow ranges, 76 μm ± 5% and 10.5 m/s ± 5%, respectively. The CHF can be seen to increase with increasing N from 591.2 to 694.6 W/cm^2 and then decrease slightly to 673.2 W/cm^2. The decrease falls within the experimental uncertainty of CHF. It can therefore be said that CHF increased by approximately 15% as N was increased by a factor of 3. Similarly, h_c increased by approximately 15% from 5.86 to about 6.60 W/cm^2 K (see Table 2). It can be concluded that increasing N helps to increase CHF and h_c.

In a study by Rini et al. [11] on saturated FC-72 spray cooling, a larger N leads to a larger q''. In that study, V and d_{32} were kept within the range of 5–10%. It was shown that as N was increased from 2.1×10^6/cm^2 s to 8.3×10^6/cm^2 s, CHF increased from 67.0 W/cm^2, by approximately 20%, to 80.0 W/cm^2, while h_c increased from 5.58 to 6.40 W/cm^2, an increase of approximately 15%. The percent increase in CHF and h_c are in good agreement with that in Rini et al. [11], although values of CHF and wetting capabilities of FC-72 and water are different.

It is of interest to know the effect of relaxing the criteria on V and d_{32}. The data set shown in Table 3 are for $V \approx 7.5$ m/s ± 20% and for $d_{32} \approx 68$ μm ± 15%. These ranges of parameters include those in Table 1. As N was varied by a factor of 4 from 5.52×10^6/cm^2 s to 29.0×10^6/cm^2 s, the value of CHF in general increased with N, as can be seen from Table 3.

The trend of increasing CHF with an increase in liquid flow rate has been observed before [5,9,13,17]. However, because $G \approx \rho\pi d_{32}^3 N/6$, it had not been determined whether the increases in CHF and h were due to individual increase in N, V, d_{32}, or a combination of them. As can be seen from Table 3, there exists no definite correlation between CHF and G. For example, consider the B250 and B50 nozzles. The nozzle with the larger G (B250; 0.00665 vs. 0.00224 kg/cm^2 s) produces a smaller CHF (671.2 vs. 761.9 W/cm^2). Similar observations can also be made by comparing results of the B250, Delavan#2, and Bete#2 nozzles, shown in Table 3. Therefore, an optimal set of spray parameters, instead of increasing G, can be used to generate large values of CHF while using small liquid mass fluxes.

It is known that near CHF many bubbles exist on the heater surface and their microlayers have nearly evaporated [11,27]. If the liquid cannot replenish the heater surface before the microlayer dry-out occurs, CHF results. As N is increased, more droplets break up the bubbles before the microlayer dries up. The action of these droplets help to replenish the heater surface with liquid and bring secondary nuclei into the liquid film, resulting in enhanced boiling heat transfer. Increasing N is also expected to enhance convection heat transfer.

Table 3
Experimental conditions and results of varying N while keeping d_{32} within 68 μm ± 15% and V within 7.5 m/s ± 20%

Nozzle type	B37	Bete#1	B200	B200	B250	B50	Delavan#2	Bete#2
Location, x (cm)	2.5	8.0	7.5	7.0	9.0	3.0	3.0	6.0
Pressure, P (psi)	50.0	120.0	80.0	60.0	80.0	100.0	80.0	60.0
N (1/cm^2 s)	5.52×10^6	11.10×10^6	12.11×10^6	13.51×10^6	15.21×10^6	25.24×10^6	26.04×10^6	29.0×10^6
G (kg/cm^2 s)	0.00172	0.00213	0.00319	0.00243	0.00665	0.00224	0.00235	0.00248
d_{32} (μm)	79.7	71.7	79.6	70.2	75.9	55.4	55.7	54.7
V (m/s)	6.9	8.2	7.1	6.0	8.7	7.3	7.9	8.0
CHF (W/cm^2)	591.2	667.8	640.6	645.1	671.2	761.9	767.1	780.2
$T_{w,CHF} - T_\infty$ (K)	100.9	106.7	107.1	107.4	104.2	108.7	108.9	109.1
h_c (W/cm^2 K)	5.86	6.26	5.98	6.01	6.44	7.01	7.04	7.15

Therefore, the overall effect of increasing N is to enhance CHF.

3.2. Effects of droplet Sauter mean diameter (d_{32})

Two sets of data were obtained to reveal the effects of d_{32} on CHF. For the first set of data (Table 4), d_{32} was varied by a factor of about 3 from 62.2 to 191.4 μm, while fixing V at approximately 6.0 m/s ± 5% and N at approximately 5.40×10^6/cm^2 s ± 5%. As can be seen from Table 4, the four nozzles with increasing magnitudes of d_{32} were in the order of B75 (62.2 μm), Bete#1 (105.0 μm), Delavan#3 (163.8 μm), and Delavan#1 (191.4 μm). However, the order of increasing CHF values was Delavan#3, B75, Delavan#1, and Bete#1, while the order for h_c was Delavan#3, Delavan#1, Bete#1, and B75. Trends of CHF and h_c with d_{32} did not appear clear, as they decrease and then increase slightly with increasing d_{32}. Similarly, increasing G (which is proportional to d_{32}^3) for fixed values of V and N, by a factor of approximately 27 does not appear to have a consistent effect on CHF.

The second set of data are presented in Table 5, where d_{32} was increased from approximately 57 to 115 μm (i.e., by a factor of approximately 2), while N and V were fixed at approximately 8.0×10^6/cm^2 s ± 10% and 7.2 m/s ± 7%, respectively. Over this range of d_{32}, G increased by a factor of more than 8. CHF increases slightly from 610.7 to 651.1 W/cm^2 (a modest 7% increase) as d_{32} and G were increased, as can be seen from Table 5. While d_{32} was varied, h_c remained relatively constant at approximately 6.0 W/cm^2 K (see Table 5).

Consequently, no clear enhancement of CHF by increasing d_{32} could be observed in spite of the accompanying increase in G by a factor of as much as 27. Increasing d_{32} might either increase or decrease h_c; the trend is not definite.

Table 6 was constructed by relaxing the ranges of V and N to 6.5 m/s ± 25% and 5.8×10^6/cm^2 s ± 30%. It can be seen in Table 6 that there is no definite trend in CHF and h_c with d_{32}, as CHF and h_c underwent several increase–decrease changes as d_{32} was increased.

Table 5
Experimental conditions and results of varying d_{32} while keeping N within 8.00×10^6/cm^2 s ± 10% and V within 7.2 m/s ± 7%

Nozzle type	B37	B200	Bete#1
Location, x (cm)	2.5	10.0	7.5
Pressure, P (psi)	50.0	80.0	80.0
d_{32} (μm)	57.3	86.5	115.7
G (kg/cm^2 s)	0.00072	0.00291	0.00687
N (1/cm^2 s)	7.30×10^6	8.62×10^6	8.50×10^6
V (m/s)	6.9	6.7	7.8
CHF (W/cm^2)	610.7	621.6	651.1
$T_{w,CHF} - T_\infty$ (K)	102.8	102.8	108.3
h_c (W/cm^2 K)	5.94	6.04	6.01

The above results of CHF are in contrast to those discussed in the Section 1, which described conflicting trends CHF and h_c with d_{32}. In those investigations, spray parameters of interest were not independently varied. It is noted that for a given nozzle d_{32} was decreased when the pressure is increased, which led to increases in V and N. Increasing N (discussed above) and/or V (shown below) leads to increases in CHF and h_c; such increases are more significant and definite than that due to increases in d_{32}.

3.3. Effects of mean droplet velocity (V)

Table 7 presents the results of varying V from 4.64 to 24.1 m/s while maintaining d_{32} and N at approximately 68.0 μm ± 2% and 15×10^6/cm^2 s ± 10%, respectively. It can be seen that as V was increased from 4.64 to 24.1 m/s the value of CHF increased from 636.7 W/cm^2, by nearly 50%, to 945.9 W/cm^2. The value of h_c also appears to increase by increasing V, from 5.94 W/cm K by approximately 40% to 8.38 W/cm K (Table 7). It is noted that the values of G, listed in Table 7, fall within a

Table 4
Experimental conditions and results of varying d_{32} while keeping N within 5.40×10^6/cm^2 s ± 5% and V within 6.0 m/s ± 5%

Nozzle type	B75	Bete#1	Delavan#3	Delavan#1
Location, x (cm)	7.5	5.0	5.5	7.5
Pressure, P (psi)	150.0	60.0	60.0	80.0
d_{32} (μm)	62.2	105.0	163.8	191.4
G (kg/cm^2 s)	0.00070	0.00343	0.01184	0.01957
N (1/cm^2 s)	5.51×10^6	5.67×10^6	5.17×10^6	5.35×10^6
V (m/s)	6.0	6.4	5.9	6.3
CHF (W/cm^2)	565.2	586.7	537.6	572.6
$T_{w,CHF} - T_\infty$ (K)	99.2	106.0	104.2	108.3
h_c (W/cm^2 K)	5.79	5.53	5.16	5.29

Table 6
Experimental conditions and results of varying d_{32} while keeping N within $5.80 \times 10^6/\text{cm}^2\,\text{s} \pm 30\%$ and V within $6.5\ \text{m/s} \pm 25\%$

Nozzle type	B37	B75	Bete#3	Bete#1	Delavan#1	B350	Delavan#3	Delavan#1
Location, x (cm)	2.5	7.5	8.0	5.0	9.5	7.0	5.5	7.5
Pressure, P (psi)	50.0	150.0	60.0	60.0	110.0	40.0	60.0	80.0
G (kg/cm^2 s)	0.00072	0.00069	0.00249	0.00343	0.00282	0.0180	0.01184	0.01957
N (1/cm^2 s)	7.30×10^6	5.51×10^6	6.00×10^6	5.67×10^6	4.34×10^6	7.28×10^6	5.17×10^6	5.35×10^6
d_{32} (μm)	57.3	62.2	92.7	105.0	107.6	135.2	163.8	191.4
V (m/s)	6.9	6.01	5.0	6.4	6.7	7.9	5.9	6.27
CHF (W/cm^2)	610.7	565.2	524.6	586.7	596.2	625.4	537.6	572.6
$T_{w,CHF} - T_\infty$ (K)	102.8	99.2	100.9	106.0	106.4	108.6	104.2	108.3
h_c (W/cm^2 K)	5.94	5.70	5.20	5.53	5.60	5.76	5.16	5.29

Table 7
Experimental conditions and results of varying V while keeping N within $15.0 \times 10^6/\text{cm}^2\,\text{s} \pm 10\%$ and d_{32} within $68.0\ \mu\text{m} \pm 2\%$

Nozzle type	B150	B200	Bete#3
Location, x (cm)	5.0	7.0	2.5
Pressure, P (psi)	40.0	60.0	80.0
V (m/s)	4.64	5.97	24.1
G (kg/cm^2 s)	0.00260	0.00244	0.00256
N (1/cm^2 s)	16.40×10^6	13.51×10^6	15.12×10^6
d_{32} (μm)	67.2	70.2	68.7
CHF (W/cm^2)	636.7	645.1	945.7
$T_{w,CHF} - T_\infty$ (K)	107.2	107.4	112.8
h_c (W/cm^2 K)	5.94	6.01	8.38

narrow range (within 5% of 0.0025 kg/cm^2 s). Therefore, the effect of V was completely isolated.

It was of interest to relax the ranges of the above-mentioned d_{32} and N, both are within approximately 30% of 70.0 μm and $17.0 \times 10^6/\text{cm}^2$ s, respectively. The effect of V on CHF and h_c can be seen in Fig. 5a and b, respectively. For simplicity, the many values in these figures are not tabulated; one is instead referred to Ref. [25] for detailed results. As can be seen from Fig. 5a and b, there exist general trends for CHF and h_c to increase with increasing V. The value of CHF increased from approximately 640 W/cm^2 at $V = 4.64$ m/s to 708.1 W/cm^2 at $V = 13.6$ m/s, and further to 945 W/cm^2 at $V = 24.1$ m/s (see Fig. 5a). For $V = 7.1$, 14.3 and 24.1 m/s, h_c values are approximately 20, 22.5 m K, and 25.0 W/cm K, respectively (see Fig. 5b).

Relaxing ranges of d_{32} and N therefore preserves the effect of V on CHF. The effect V is clearly more pronounced than those of d_{32} and N discussed above. Again, depending on how widely the other parameters are varied, the effect of varying d_{32} by a factor of more than 3 might either increase or decrease CHF, or did not have a significant effect. Increasing N by a factor of 2–4 has a moderate effect on CHF (an increase of 18–30% in this study).

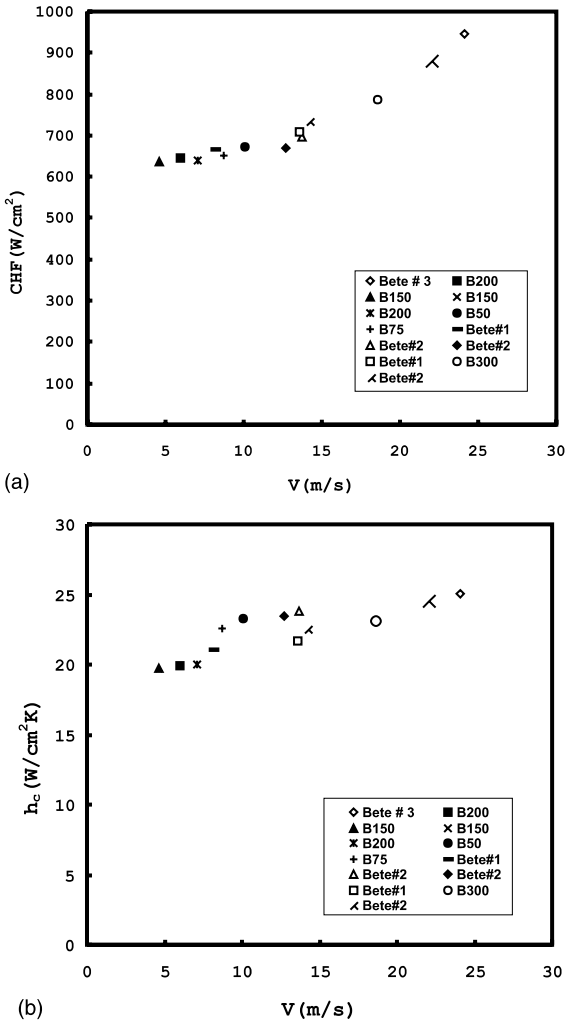

Fig. 5. (a) CHF and (b) h_c vs. spray velocity (V) for V varied by a factor of 4 while d_{32} and N were more relaxed (maintained within 40%) than those in Table 7. For nozzle types, see Tables 1–9.

From the above discussion, it is believed that a combination of increased N and increased V would most effectively enhance heat transfer and CHF. Increasing N is expected to increase the number of secondary nuclei [14]. This in turn leads to an increased nucleate heat transfer, which is more effective than single-phase convection. For a given N, droplets with larger V would bring the entrained secondary nuclei closer to the heater surface, enhancing the evaporation into the nuclei and heat transfer. As a result of increasing V, the mixing and convective heat transfer are also enhanced. This may help to explain why increasing V is more effective than increasing N in enhancing CHF. Because $N = nV$, sprays with larger V and smaller n result in higher values of CHF than those with smaller V and larger n for a given value of N.

3.4. Further results and discussion on the dominating effect of droplet velocity (V)

Chow and co-workers [8,13] demonstrated that smaller orifice nozzles provide larger values of CHF than larger nozzles for similar flow rates. It was reasoned that, for a given flow rate, smaller droplets lead to a larger value of Nd_{32}^2 (which is $\propto 1/d_{32}$ because $N \propto 1/d_{32}^3$). Therefore, sprays from smaller nozzles create a larger impact/wetted area per unit time on the surface, which in turn prevents dry-out until a higher heat flux is supplied to the surface. However, the effect of d_{32} in increasing CHF appears to be insignificant, as discussed above. Therefore, the enhancement of CHF is achievable by increasing N based on Chow et al.'s reasoning, which was already demonstrated above. If one is to fix V, then an increase in N is accompanied by an increase in G. Effects of G and N may therefore be inseparable. As an effort to resolve this dilemma, experimental conditions listed in Table 8 were investigated.

To determine the effect of G for given values of V, consider the following cases in Table 8: Bete#1 with $x = 8.0$ cm and $P = 120$ psig and B75 with $x = 6.0$ cm and $P = 160$ psig. The velocities for them are within approximately 5% of each other, while the mass flow rates are 0.0021 and 0.0049 kg/cm^2 s, by a factor of 4, and values of d_{32} and N are different by more than 20%. The values of CHF for these two experimental conditions are within approximately 2% of each other (approximately 653 and 668 W/cm^2, as can be seen from Table 8). The effect of V (similar values of V lead to similar values of CHF, as discussed above) appears to be more dominant than those of G, d_{32}, and N.

Another example in Table 8 demonstrating nearly equal values of CHF as a result of nearly equal magnitudes of V comprises of Bete#1 with $x = 5.0$ cm and $P = 80$ psig and Bete#2 with $x = 9.5$ cm and $P = 120$ psig. These two experimental conditions have nearly equal velocities, 13.6 and 13.7 m/s, respectively, while G, d_{32}, and N are again different as shown in Table 8 (e.g., values of G are 0.0014 vs. 0.0034 kg/cm^2, differing by a factor of 2). It is seen from Table 8 that the values of CHF for these two experimental conditions are nearly equal, approximately 696 W/cm^2 for the Bete#2 nozzle and 708 W/cm^2 for the Bete#1 nozzle (i.e., within 2% of each other).

The results of Bete#3 with $x = 2.5$ cm and $P = 80$ psig and B150 with $x = 5$ cm and $P = 40$ psig in Table 8 were also reported in Table 7, demonstrating a 50% increase in CHF by increasing V by a factor of 4. It is noted that for these two nozzles values of other spray parameters are within narrow ranges. Similar result can be observed for Bete#1 with $x = 5.0$ cm and $P = 80$ psig and B200 with $x = 7.5$ cm and $P = 80$ psig (see Table 8). Their values of G, N, d_{32} were held nearly equal at approximately 0.0033 kg/cm^2 s, 11.5×10^6/cm^{2}s, and 80 μm, respectively, while their velocities differs by a factor of approximately 2, 7.1 m/s (B200 nozzle) vs. 13.6 m/s (Bete#1 nozzle). As a result, CHF increases with V from 640 to 708 W/cm^2, by about 10%. The effect of increasing V on CHF enhancement is clearly seen.

A further example consists of the conditions of Bete#2 with $x = 3.0$ cm and $P = 120$ psig and B50 with $x = 8.5$ cm and $P = 160$ psig (again, see Table 8). Their values of G and N were held nearly equal at approximately

Table 8
Experimental results demonstrating the dominant effects of V on CHF over a wide range of d_{32} and N

Nozzle type	Bete#3	B150	Bete#1	B200	Bete#2	Bete#2	B50	Bete#1	B75
Location, x (cm)	2.5	5.0	5.0	7.5	9.5	3.0	8.5	8.0	6.0
Pressure, P (psi)	80.0	40.0	80.0	80.0	120.0	120.0	160.0	120.0	160.0
V (m/s)	24.1	6.0	13.6	7.1	13.7	22.1	10.1	8.2	8.7
G (kg/cm^2 s)	0.0026	0.0026	0.0034	0.0032	0.0014	0.0039	0.0038	0.0021	0.0049
N (10^6/cm^2 s)	15.12	16.40	11.21	12.11	14.43	20.14	18.83	11.10	14.77
d_{32} (μm)	68.7	70.2	83.7	79.6	57.4	90.3	72.6	71.9	85.9
CHF (W/cm^2)	945.7	636.7	708.1	640.6	695.8	880.2	673.2	667.8	652.7
$T_{w,CHF} - T_\infty$ (K)	112.8	107.2	107.7	107.1	104.2	110.7	103.9	106.7	103.9
h_c (W/cm^2 K)	8.38	5.94	6.57	5.98	6.67	7.95	6.48	6.26	6.28

Table 9
Rearrangement of Table 6 to demonstrate the dominant effect of V

Nozzle type	Bete#3	Delavan#3	B75	Delavan#1	Bete#1	Delavan#1	B37	B350
Location, x (cm)	8.0	5.5	7.5	7.5	5.0	9.5	2.5	7.0
Pressure, P (psi)	60.0	60.0	150.0	80.0	60.0	110.0	50.0	40.0
V (m/s)	5.0	5.9	6.0	6.3	6.4	6.7	6.9	7.9
G (kg/cm^2 s)	0.00249	0.01184	0.00069	0.01957	0.00343	0.00282	0.00072	0.0180
N (1/cm^2 s)	6.00×10^6	5.17×10^6	5.51×10^6	5.35×10^6	5.67×10^6	4.43×10^6	7.30×10^6	7.28×10^6
d_{32} (μm)	92.7	163.8	62.2	191.4	105.0	107.6	163.8	135.2
CHF (W/cm^2)	524.6	537.6	565.2	572.6	586.7	596.2	610.7	625.4
h_c (W/cm^2 K)	5.20	5.16	5.70	5.29	5.53	5.60	5.94	5.76

0.0038 kg/cm^2 s and 19.5×10^6/cm^2 s, respectively. Although the Bete#2 nozzle provides a slightly larger d_{32} (90.2 vs. 79.6 μm), this effect is expected to be insignificant as discussed earlier. It is worth noting that the velocity using the B50 nozzle is larger than that of the Bete#2 nozzle (22.1 vs. 10.1 m/s) and yields a CHF of 880 W/cm^2, compared to 673 W/cm^2 of the B50 nozzle.

The dominant effect of V on CHF shown in Table 7 and Fig. 5a, has again been demonstrated using Table 8 in the following two ways. First, keeping V nearly equal while varying other spray parameters produced nearly equal values of CHF. Secondly, varying V while keeping other spray parameters nearly equal produced different values of CHF.

The dominant effect of V is further seen by examining the results shown in Table 6. For clarity, Table 6 was rearranged to generate Table 9. The nozzles and their spray conditions are arranged from left to right in Table 9 with increasing velocity. It is noted that the values of G, d_{32}, and N were varied by factors of approximately 27, 3, and 1.7, respectively, and that they are not listed in order. In Table 9, the velocity increase was incremental, from 5.0 to 7.9 m/s, a 60% increase. CHF can be seen to increase with each increment of the seven increments in V, from approximately 525 to 625 W/cm^2, approximately a 20% increase. If one rearranges Table 9 so that each of G, d_{32} and N is in increasing order (already done in Table 6 for d_{32}), CHF would not consistently increase with increasing values of these parameters. It is worth further noting that variations in these parameters are significantly larger than that in V. These observations should clearly confirm that V is a more dominating factor in determining CHF than the other spray parameters. In an experiment using mono-dispersed droplets, similar effect of V was observed in the nucleate heat transfer regime and not in film boiling regime [23].

Following the above discussion, one might expect the value of CHF to fall within a narrow range if G, N, d_{32}, and V all fall within narrow ranges. To demonstrate, consider the following nozzles in Table 3: B50 with $x = 3.0$ cm and $P = 100.0$ psi, Delavan#2 with $x = 3.0$ cm and $P = 100.0$ psi, and Bete#2 with $x = 6.0$ cm and $P = 60.0$ psi. The spray parameters for these three nozzles all fall within narrow ranges with $G = 0.00224$–0.00248 kg/cm^2 s, $N = 25.2 \times 10^6$/cm^2 s to 29.0×10^6/cm^2 s, $d_{32} = 54.7$–55.7 μm, and $V = 7.3$–8.0 m/s. The values of their CHF similarly fall with a very narrow range: 761.9–780.2 W/cm^2 (i.e., within 3%, which is less than the experimental uncertainty). Considering that different vendors provided these nozzles, this result and those discussed earlier should not be attributed to coincidence.

3.5. Effects of N vs. V

Since $N = nV$, it is reasonable to associate the effects of N and V because they might appear to be proportional to each other. However, it is possible to have d_{32} and N kept in narrow ranges while varying V, as discussed above. This can be achieved by varying n and V in so that N remains constant. The independent effect of V has thus been shown in Table 7 and part of Table 3. It can therefore be said that, to increase CHF, one would rather use a dilute spray (small n) with large droplet velocity than a dense spray (large n) with low velocities.

4. Conclusion

Spray parameters (flow rate, droplet size, droplet flux, and droplet velocity) in spray cooling were independently varied, and their effects on critical heat flux and heat transfer were studied, using nozzles from different manufacturers. The findings are summarized as follows.

1. The droplet velocity (V) had the most dominant effect on CHF and the heat transfer coefficient, followed by the droplet flux (N). The Sauter mean diameter (d_{32}) did not appear to have a definite effect.
2. By increasing V, CHF and h_c were increased. This trend was observed whether all other spray parame-

ters were kept within narrow ranges or relaxed to wider ranges.

3. Increasing N resulted in an increase in CHF and h_c when other parameters are kept in narrow ranges. This general trend was also observed, with a few exceptions, when the range of other spray parameters was relaxed. The exception can be attributed to, for example, the fact that V is a dominant factor. A more relaxed range of V would shift the effect being studied from that of N to that of V.
4. To increase CHF for a given N, a dilute spray with large droplet velocity appears to be more effective than a dense spray with low velocities.

Acknowledgements

This research has been supported by the National Science Foundation (NSF) Division of Chemical and Thermal Systems (Grant numbers CTS-9813959 and CTS-9616344).

References

[1] A. Bar-Cohen, State-of-the-art and trends in the thermal packaging of electronic equipment, J. Electron. Packaging 114 (1992) 257–270.
[2] R.G. Waters, Diode laser degradation mechanisms: a review, Prog. Quant. Electron. 15 (1983) 153–174.
[3] J. Yang, L.C. Chow, M.R. Pais, Nucleate boiling heat transfer in spray cooling, J. Heat Transfer 118 (1996) 668–671.
[4] X.Q. Chen, L.C. Chow, M.S. Sehmbey, Thickness of film produced by a pressure atomizing nozzle, in: 30th AIAA Thermophysics and Heat Transfer Conference, San Diego, CA, Paper No. AIAA-95-2103, 1995.
[5] M.R. Pais, L.C. Chow, E.T. Mahefkey, Surface roughness and its effect on the heat transfer mechanism in spray cooling, J. Heat Transfer 114 (1992) 211–219.
[6] M.S. Sehmbey, L.C. Chow, O.J. Hahn, M.R. Pais, Effect of spray characteristics on spray cooling with liquid nitrogen, AIAA J. Thermophys. Heat Transfer 9 (1995) 757–765.
[7] M.S. Sehmbey, M.R. Pais, L.C. Chow, Effect of surface material properties and surface characteristics in evaporative spray cooling, AIAA J. Thermophys. Heat Transfer 6 (1992) 505–512.
[8] M.S. Sehmbey, L.C. Chow, O.J. Hahn, M.R. Pais, Spray cooling of power electronics at cryogenic temperatures, AIAA J. Thermophys. Heat Transfer 9 (1995) 123–128.
[9] K.A. Estes, I. Mudawar, Correlation of Sauter mean diameter and critical heat flux for spray cooling of small surfaces, Int. J. Heat Mass Transfer 38 (1995) 2985–2996.
[10] D.P. Rini, R.-H. Chen, L.C. Chow, Bubble behavior and nucleate boiling heat transfer in saturated FC-72 spray cooling, J. Heat Transfer 24 (2002) 63–72.
[11] D.P. Rini, R.-H. Chen, L.C. Chow, Bubble behavior and heat transfer mechanism in FC-72 pool boiling, Exp. Heat Transfer 14 (2001) 27–44.
[12] D. Nguyen, R.-H. Chen, L.C. Chow, C. Gu, Effects of heater orientation and confinement on liquid nitrogen pool boiling, AIAA J. Thermophys. Heat Transfer 14 (2000) 109–111.
[13] L.C. Chow, M.S. Sehmbey, M.R. Pais, High heat flux spray cooling, Ann. Rev. Heat Transfer 8 (1997) 291–318.
[14] L.A. Kopchikov, G.I. Voronin, T.A. Kolach, D.A. Labuntsov, P.D. Lebedev, Liquid boiling in a thin film, Int. J. Heat Mass Transfer 12 (1969) 791–796.
[15] S. Toda, A study of mist cooling, 1st report: investigation of mist cooling, Heat Transfer – Jpn. Res. 1 (1972) 39–50.
[16] S. Toda, A study of mist cooling, 2nd report: theory of mist cooling and its fundamental experiments, Heat Transfer – Jpn. Res. 3 (1974) 1–44.
[17] S. Toda, H. Uchida, Study of liquid film cooling with evaporation and boiling, Heat Transfer – Jpn. Res. 2 (1973) 44–62.
[18] M. Monde, Critical heat flux in saturated forced convection boiling on a heated disk with impinging droplets, Heat Transfer – Jpn. Res. 8 (1979) 54–64.
[19] D.E. Tilton, Spray cooling, Ph.D. Dissertation, University of Kentucky, Lexington, KY, 1989.
[20] P.J. Halvorson, R.J. Carson, S.M. Jeter, S.I. Abdel-Khalik, Critical heat flux limits for a heated surface impacted by a stream of liquid droplets, J. Heat Transfer 116 (1994) 679–685.
[21] S.C. Yao, Dynamics and heat transfer of impacting sprays, Ann. Rev. Heat Transfer 5 (1994) 351–382.
[22] J.D. Bernardin, I. Mudawar, Film boiling heat transfer of droplet streams and sprays, Int. J. Heat Mass Transfer 40 (1997) 2579–2593.
[23] S.C. Yao, K.J. Choi, Heat transfer experiments of monodispersed vertically impacting sprays, Int. J. Multiphase Flow 13 (1987) 639–648.
[24] K.J. Choi, S.C. Yao, Mechanisms of film boiling heat transfer of normally impacting spray, Int. J. Heat Mass Transfer 30 (1987) 311–318.
[25] J.E. Navedo, Parametric effects of spray characteristics on spray cooling heat transfer, Ph.D. Dissertation, University of Central Florida, Orlando, FL, 2000.
[26] Dantec PDPA Manual, Reproduced and Copyrighted by Dantec Corporation, 1995.
[27] S. Nishio, T. Gotoh, N. Nagai, Observation of boiling structure in high heat flux boiling, Int. J. Heat Mass Transfer 41 (1998) 3191–3201.